Desalination and Water Treatment
www.deswater.com
doi: 10.1080/19443994.2013.794012

52 (2014) 248–256
January

Taylor & Francis
Taylor & Francis Group

Modeling of disperse dye adsorption onto bamboo-based activated carbon in fixed-bed column

A.A. Ahmad[a,*], A. Idris[a], B.H. Hameed[b]

[a]*Faculty of Engineering, Department of Chemical and Environmental Engineering, University Putra Malaysia, 43400 UPM, Serdang, Malaysia*
Tel. +603-89466302; Fax: +603-86567120; email: abdulbari@eng.upm.edu.my
[b]*School of Chemical Engineering, Engineering Campus, University Science Malaysia, Nibong Tebal, 14300, Penang, Malaysia*

Received 9 June 2012; Accepted 6 March 2013

ABSTRACT

The adsorption of I.C. Disperse Orange 30 (DO30) onto bamboo-based activated carbon (BMAC) was investigated in a fixed-bed column. The experiments were conducted to study the effect of important parameters: bed depth (4–8 cm), flow rate (10–30 mL/min), and inlet DO30 concentrations (50–200 mg/L). The experimental results showed that the breakthrough time decreased with increased flow rate and inlet concentration and it decreased bed height. The highest bed capacity of 39.97 mg/g was obtained to use 100 mg/L inlet DO30 concentration, 8 cm bed height, and 10 mL/min flow rate. Adams–Bohart, bed depth service time (BDST), Thomas and Yoon–Nelson models were applied to predict the breakthrough point using linear regression and to determine the characteristic parameters of the column. Thomas model prediction was in a very good agreement with the experimental results at all the process parameters. The study indicates that it is very suitable for BMAC column design.

Keywords: Disperse dye; Activated carbon; Adsorption; Breakthrough; Modeling

1. Introduction

Dye effluents with persistent color carcinogens toxic to micro-organisms, aquatic life, and human beings [1]. Dyes are difficult to degrade as they are generally stable to light oxidizing agent and are resistant to aerobic digestion [2]. There are more than 100,000 different commercial dyes and pigments exist with over 7×10^5 tonnes of dyestuff produced annually [3]. The exact data on the quantity of dyes discharge in the environment are also not available. Synthetic dyes are extensively used in many fields: various branches of the textile industry [4], the leather tanning industry [5] paper production [6], food technology [7], agricultural research [8], light-harvesting arrays [9], photoelectrochemical cells [10], and hair colorings [11].

Disperse dyes are widely used in a variety of industries, such as textiles, paper, and leather. Disperse dyes are nonionic aromatic compounds, scarcely soluble in water. But it is soluble in organic solvent. The majority of disperse dyes are azo and anthraquinone dyes. These dyes can be applied to synthetic fibers, such as polyester, nylon, acetate, cellulose, and acrylic [12]. Textile industries' effluent contains many dyes. These contain carcinogen and mutagen

*Corresponding author.

chemicals, such as benzidine, metals, etc. and causes serious environmental problems [13].

Currently, several physical or chemical processes such as coagulation, precipitation, sedimentation, ultrafiltration, ozonation, oxidation, and reverse osmosis are used to treat wastewaters [14]. However, adsorption is considered superior as compared to other traditional treatment methods, because it is easily available, simple design, highly efficient, ease in operation, and ability to treat dyes in more concentrated forms [15]. Adsorption does not affect the formation of harmful substances and insensitivity to toxic pollutants. Activated carbon is the most widely used adsorbent due to its high adsorption abilities for a large number of organic compounds [16]. In addition, the chemical nature of their surfaces enhances adsorption. However, commercially available activated carbons are generally expensive because of running costs, thereby limited in use. Consequently, there is a growing interest in recent years, to produce activated carbon and bio-char from renewable sources and inexpensive materials [17].

Batch reactors are easy to use in the laboratory study, but less convenient for industrial applications. Batch experiments are usually done to measure the effectiveness of adsorption to remove specific adsorbates and determine the maximum adsorption capacity. The continuous adsorption in fixed-bed column is often desired from industrial point of view. Continuous adsorption is considered useful in large-scale industrial wastewater treatment because of their simplicity, handling, regeneration capacity, and ease of operation [18]. On the other hand, fixed-bed columns are widely used in various chemical industries because of their operation [19]. The performance of fixed-bed column is described through the concept of the breakthrough curve. The time for breakthrough appearance and the shape of the breakthrough curve are very important characteristics to determine the operation and the dynamic response of an adsorption column [20]. Furthermore, the data analyzed by the column adsorption provide valuable information for the design and operation of wastewater treatment plants. In addition, the adsorption mechanism is determined by the fitting results of the breakthrough curves [21].

Therefore, the focus of this research was to evaluate the adsorption potential of the bamboo-based activated carbon (BMAC) in removing I.C. Disperse Orange 30 (DO30) from aqueous solutions using a laboratory scale fixed-bed column. In order to analyze the column dynamics in the adsorption process, the effect of flow rate, influent concentration, and activated carbon bed height on the breakthrough curves was observed. The breakthrough curves for the adsorption of DO30 were analyzed by using Adams–Bohart, bed depth service time (BDST), Thomas and Yoon–Nelson models.

2. Materials and methods

2.1. Adsorbate

C.I. 30 dye Disperse Orange, 4-((2,6-Dichloro-4-nitrophenyl)azo)-N-(cyanoethyl)-N-(acetoxyethyl) (Scheme 1) supplied by Sigma–Aldrich (M) Sdn Bhd, Malaysia was used as an adsorbate and was not purified prior to use. Distilled water was used to prepare all the solutions. DO30 has a chemical formula of $C_{19}H_{17}Cl_2N_5O_4$, with molecular weight of 450.27 g/mol.

2.2. Preparation and characterization of activated carbon

Bamboo waste (BM) used for the preparation of activated carbon (BMAC) was collected from a local furniture shop in Penang State, Malaysia. The procedure used to prepare the activated carbon referred to the previous work of the research [22], the BM was briefly washed with hot distilled water to remove dust-like impurities. It was dried at 105°C, grounded, and sieved to discrete sizes. Activation of the phosphoric acid impregnated precursor was carried out at temperature of 500°C for 2 h under purified nitrogen (99.995%) flow (150 cm^3/g) at a heating rate of 10°C/min in a horizontal tubular furnace. After activation, the sample was cooled down to room temperature with the same heating rate and washed sequentially several times with hot distilled water (70°C) until the pH of the washing solution reached 6–7. Finally, the sample was dried in an oven at 110°C for 24 h and then stored in plastic containers.

Surface morphology and the presence of porosity of the activated carbon prepared in this work were studied by using scanning electron microscopy analy-

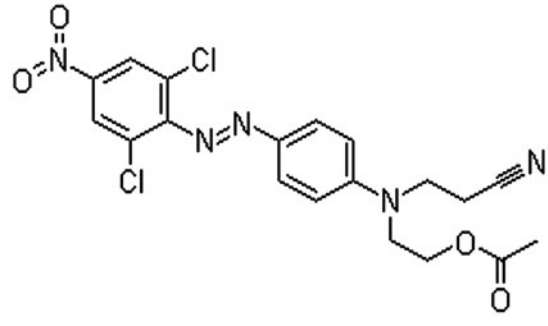

Scheme 1. Chemical structure of C.I. Disperse Orange 30 (DO30).

sis. Surface physical properties of the BMAC were carried out by N_2 adsorption at 77 K using ASAP 2020 Micromeritics instrument. In addition, the surface functional groups of the prepared activated carbon were detected by Fourier transform infrared spectrometer in the scanning range of 4,000–400 $cm.^{-1}$

2.3. Experimental set-up

The fixed-bed column was made of a Pyrex glass tube of 1.2 cm inner diameter and 19.5 cm height. At the bottom of the column, a stainless steel sieve was attached followed by a layer of glass wool. A known quantity of the prepared activated carbon was packed in the column to yield the desired bed height of the adsorbent 4, 6, and 8 cm. The column was then filled up with glass beads in order to provide a uniform flow of the solution through the column. Dye solution of known concentrations at pH 6.3 ± 0.2 was pumped upward through the column at a desired flow rate controlled by a peristaltic pump (Masterflex, Cole-Parmer Instrument Co.). The operational conditions of this column experiment are shown in Table 1. The DO30 solutions at the outlet of the column were collected at regular time intervals and the concentration was measured using a double beam UV–Visible spectrophotometer (Shimadzu, Japan) at 425 nm. Calibration curves were plotted between absorbance and concentration of the dye solution.

The time for breakthrough appearance and the shape of the breakthrough curve are very important characteristics to determine the operation and the dynamic response of an adsorption column. The evaluation of the column performance was conducted by plotting DO30 relative concentration. It is defined as the ratio of DO30 concentration in effluent to DO30 concentration in an influent (C_t/C_o), as a function of flow time (t, min). The total adsorbed DO30 (q_t, mg) in the column for a given solute concentration and flow rate is calculated from the following equation:

$$q_{total} = \frac{Q}{1,000} \int_{t=0}^{t=t_{total}} C_{ad} dt \quad (1)$$

where Q (mL/min) is the volumetric flow rate and C_{ad} (mg/L) is the adsorbed DO30 concentration (inlet concentration, C_o—outlet concentration, C_t), and t_{total} is the total flow time (min).

Equilibrium DO30 uptake in the column or maximum capacity of the column (q_{eq}) was defined by Eq. (2) as the total amount of dye adsorbed (q_{total}) per g of the adsorbent (w) at the end of the total flow time [23].

$$q_{eq} = \frac{q_{total}}{w} \quad (2)$$

Table 1
Operational parameters of the column experimental set up

Flow rate (mL/min)	10–30
Column height (cm)	19.5
Internal diameter (cm)	1.2
Area of column (cm^2)	1.131
Column material	Pyrex glass
Bed height (cm)	4, 6, 8
Bed volume (cm^3)	4.524, 6.786, 9.048
Mass of adsorbent (g)	2.74, 3.65, 4.53
Type of pump	Peristaltic pump
Particle size range (μm)	200–300
Solution of concentrations (mg/L)	50, 100, 200
Temperature (°C)	26 ± 2
pH	6.3 ± 0.2
Mode of flow	Up flow (without effluent recycling)

3. Breakthrough curve modeling

Bohart-Adams [24] model was used for the initial part of the breakthrough curve. Its overall approach is now being applied successfully in quantitative description of other systems. The mathematical equation of the model can be written as:

$$\ln \frac{C_t}{C_o} = k_{AB} C_o t - k_{AB} N_o \frac{Z}{F} \quad (3)$$

where C_o and C_t (mg/L) are the inlet and effluent concentration. k_{AB} (L/mg min) is the kinetic constant, F (cm/min) is the linear velocity calculated by dividing the flow rate in the column section area, Z (mm)is the bed depth of column and N_o (mg/L) is the saturation concentration. A linear plot of ln C_t/C_o against time (t) was determined by the values of k_{AB} and N_o from the intercepts and slopes of the plot.

The BDST [25] model is used only for the description of the initial part of the breakthrough curve. The limit is to the breakpoint or 10–50% of the saturation points [26]. This model was focused on the estimation of characteristic parameters, such as the maximum adsorption capacity and kinetic constant. The BDST model which was formulated by Hutchins [25] elucidates a relation between the service time and the

packed-bed depth of the column and is expressed as under:

$$C_o t = \frac{N_o h}{u} - \frac{1}{k}\ln\left[\frac{C_o}{C_t} - 1\right] \quad (4)$$

where C_o (mg/L) is the influent concentration, C_t (mg/L) is the effluent concentration at the time t, K is the adsorption rate constant (L/mg min), N_o is the adsorption capacity (mg/L), h is the bed height (mm), u is the linear flow rate (mL/min), and t is the service time to breakthrough (min). A linear plot of $C_o t$ against $\ln[(C_o/C_t)-1]$ was employed to determine values of N_o and K from the intercept and slope of the plot.

The expression developed by Thomas [27] calculates the maximum solid phase concentration of the solute on the adsorbent and the adsorption rate constant for a continuous adsorption process in column. The linearized form of the model is given as:

$$\ln\left(\frac{C_o}{C_t} - 1\right) = \frac{k_{Th} q_o w}{Q} - k_{Th} C_o t \quad (5)$$

where k_{Th} (mL/min mg) is the Thomas rate constant, q_o (mg/g) is the equilibrium effluent uptake per g of the adsorbent, C_o (mg/L) is the inlet effluent concentration; C_t (mg/L) is the outlet concentration at time t; W (g) the mass of adsorbent, Q (mL/min) the flow rate, and t_{total} (min) stands for flow time. The value of C_t/C_o is the ratio of outlet and inlet effluent concentrations. A linear plot of $\ln[(C_o/C_t)-1]$ against time (t) was employed to determine values of k_{Th} and q_o from the intercepts and slopes of the plot.

Yoon–Nelson [28] model was used to investigate the breakthrough behavior of adsorption of DO30 on BMAC. The linearized model for a single component system is expressed as under:

$$\ln\frac{C_t}{C_o - C_t} = k_{YN} t - \tau k_{YN} \quad (6)$$

where k_{YN} (1/min) is the rate velocity constant, τ (min) is the time required for 50% adsorbate breakthrough. A linear plot of $\ln [C_t/(C_o - C_t)]$ against sampling time (t) was determined by the values of k_{YN} and $\tau$from the intercept and slope of the plot.

4. Results and discussion

4.1. Characterization of BMAC

The SEM image of the derived activated carbon is referred to previous work of the research [22]. Many large pores in a honeycomb shape were clearly found on the surface of the activated carbon. The well-developed pores had led to the large surface area and porous structure of the activated carbon. The BET surface area, Langmuir surface area, total pore volume, and average pore diameter of the prepared activated carbon were 988.23 m^2/g, 1,561.164 m^2/g, 0.696 cm^3/g, and 2.82 nm, respectively. The FTIR spectrum of the prepared activated carbon is referred to the previous work of the research [22]. The main surface functional groups present in the derived activated carbon were quinone and aromatic rings.

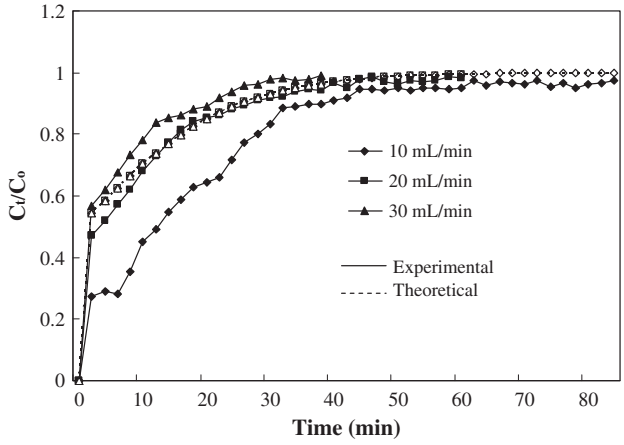

Fig. 1. Experimental and theoretical breakthrough curve from Thomas model at different flow rates, experimental conditions: pH, 6.3 ± 0.2; bed height, 80 mm; adsorbate concentration, 100 mg/L.

4.2. Effect of flow rate

The effect of flow rate on DO30 adsorption by BMAC was investigated to vary the flow rate from 10 to 30 mL/min and to keep the inlet DO30 concentration (100 mg/L) and bed depth (80 mm) constant. The effect of flow rate on breakthrough performance at the above operating conditions is shown in Fig. 1. It is mentioned in figure where the adsorption efficiency is higher at lower flow rate. The breakthrough curve becomes steeper when the flow rate is increased at the breakpoint time. This is explained by the fact that at lower flow rate, the residence time of the adsorbate is more and hence the adsorbent gets more time to bond with the dye efficiently. In other words, if the residence time of the solute in the column is not large enough for adsorption equilibrium to reach to the given flow rate, the DO30 solution leaves the column before equilibrium occurs. Equilibrium DO30 uptakes (q_e), breakpoint time and exhaustion time or the total time at different flow rates are presented in Table 2.

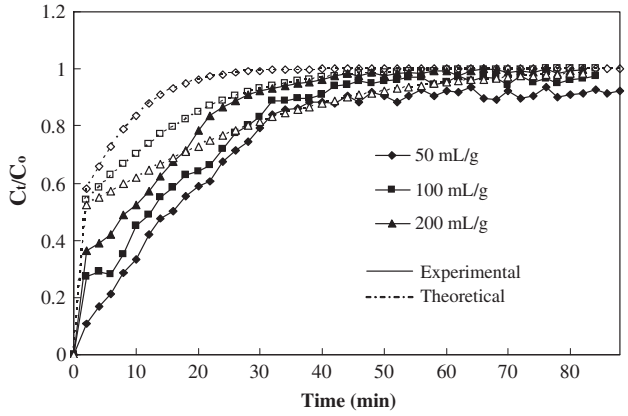

Fig. 2. Experimental and theoretical breakthrough curve from Thomas model at different inlet concentrations, experimental conditions: pH, 6.3 ± 0.2; bed height, 60 mm; flow rate 10 mL/min.

An earlier breakthrough and exhaustion time were observed in the profile, when the flow rate was increased to 30 mL/min. It was also observed that the adsorbent gets saturated easily at higher flow rates. The optimum uptake capacity for flow rate of 10, 20, and 30 mL/min were found to be 29.33, 20.71, and 12.64 mg/g, respectively (Fig. 1). Similar effect of the adsorption of methylene blue by phoenix tree leaf powder in a fixed-bed column [29] and jackfruit leaf powder was observed [30].

4.3. Effect of inlet concentration

Column experiments were carried out to vary the DO30 concentration between 50, 100, and 200 mg/L to determine the effect of DO30 concentration on the performance of the breakthrough curve. During these experiments, other parameters like bed height (60 mm) and flow rate (10 mL/min) were kept constant. The adsorption breakthrough curves were obtained for adsorbate concentrations of 50, 100, and 200 mg/L. It is shown in Fig. 2. At the highest DO30 concentration of 200 mg/L, the activated carbon bed was exhausted in the shortest time of less than 82 min leading to the earliest breakthrough. With an increase in inlet DO30 concentration from 50 to 200 mg/L, the uptake and total DO30 were found to decrease from 29.33 to 27.33 mg/g, respectively (Table 2). The breakpoint time decreased with increasing the inlet concentration as the binding sites became more quickly saturated in the column. This indicated that an increase in the concentration could modify the adsorption rate through the bed. A decrease in the initial DO30 concentration gave an extended breakthrough curve to indicate that a higher volume of the solution could be treated. This was due to the fact that a lower concentration gradient caused a slower transport due to a decrease in the diffusion coefficient or mass transfer coefficient. These results were in agreement with those reported in previous studies [30–32].

Table 2
Column data parameters obtained at different initial DO30 concentrations, bed heights and flow rates ($T = 26 \pm 2^{o}C$, pH = 6.3 ± 0.2)

Initial DO30 concentration (mg/L)	Bed height (mm)	Flow rate (mL/min)	Complete bed exhaustion time (min)	Bed capacity, q_{eq} (mg/g)
50	60	10	88	29.33
100	60	10	84	28.36
200	60	10	82	27.33
100	40	10	78	22.56
100	80	10	90	39.97
100	60	20	60	20.71
100	60	30	38	12.64

4.4. Effect of bed height

In order to find out the effect of bed height on the breakthrough curve, the adsorbate solution having DO30 concentration 100 mg/L and flow rate 10 mL/min was passed through the adsorption column by varying the bed height. Fig. 3 represents the performance of breakthrough curves at bed heights of 40, 60, and 80 mm. With an increase in bed height, the throughput volume increased which due to higher

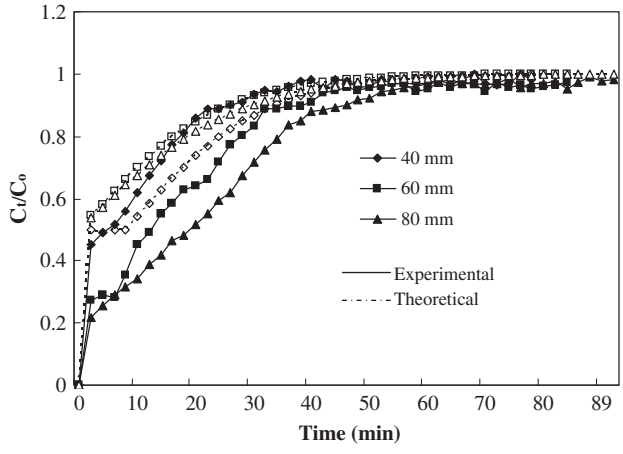

Fig. 3. Experimental and theoretical breakthrough curve from Thomas model at different bed heights, experimental conditions: pH, 6.3 ± 0.2; flow rate, 10 mL/min; inlet concentration, 100 mg/L.

contact time. At a relatively lower contact time, the curve was steeper showing the faster exhaustion of the bed. The adsorption uptakes of DO30 were found to be 22.56, 28.36, and 39.97 mg/g when the bed heights were 40, 60, and 80 mm and the complete bed exhaustion time (min) were 78, 84, and 90 min, respectively (Table 2). The increase in dye uptake capacity with the increase of bed height in the fixed-bed column was due to increased surface area of the adsorbent, which provided more binding sites for the adsorption. As it is expected in an increased bed resulted in high volume of DO30 solution treated and high removal of DO30. This observation is in agreement with earlier reported by other studies [32–34].

4.5. Modeling

4.5.1. Adams–Bohart model

Adams–Bohart model was applied on experimental data for the description of the initial part of the breakthrough curve. This approach focused on the estimation of characteristic parameters, such as maximum adsorption capacity (N_o) and the mass transfer coefficient (k_{AB}). In the present study, the range of time was considered from the beginning to the end of the breakthrough curve. The $\ln(C_t/C_o)$ values were plotted against t at different flow rates, bed heights, and initial DO30 concentrations. The mass transfer coefficient (k_{AB}) and saturation concentration (N_o) values were calculated from the slope and intercept of the curve, respectively. After applying Eq. (3) to the experimental data, the parameters were obtained for the relative concentration region up to 0.5, i.e. up to 50% breakthrough, for all breakthrough curves using linear. For all breakthrough curves, respective values of N_o, and k_{AB} were calculated and presented in Table 3 together with the correlation coefficients ($R^2 > 0.75$). From Table 3, the values of N_o at all conditions have no significant difference. The values of k_{AB} decrease with both DO30 concentration and on increasing flow rate, but it increase when bed depth increase. This shows that the overall system kinetics was dominated by external mass transfer in the initial part of adsorption in the column [23].

4.5.2. BDST

The BDST model is based on physically measurement of the capacity of the bed at different breakthrough values. This simplified design model ignores the intraparticle mass transfer resistance and external film resistance such that the adsorbate is adsorbed onto the adsorbent surface directly [35]. The estimated values of characteristic parameters, like K and N_o along with the correlation coefficients ($R^2 > 0.89$) are presented in Table 3. The BDST model parameters are helpful to scale up the process for other flow rates without further experimental runs [31].

4.5.3. Thomas model

The experimental data were fitted to the Thomas model to determine the Thomas rate constant (k_{TH}) and maximum solid phase concentration (q_o). The k_{TH} and q_o and R^2 (0.95–0.99) are listed in Table 3. The correlation of C_t/C_o and t according to Eq. (5) is significant. From the regression coefficient (R^2), it can be concluded that the experimental data fitted well to the Thomas model. As flow rate increased the k_{TH} value increased, whereas the value of q_o decreased with the increase in flow rate. From Table 3, as the influent concentration increased, the value of q_o decreased. So, higher flow rate and higher influent concentration have a disadvantage for the adsorption of DO30 on the BMAC column. Similar trend is also observed by Aksu and Gonen [23].

The predicted curves at various experimental conditions according to the Thomas model at flow rate, bed height, and influent DO30 concentrations are shown in Figs. 1–3, respectively. It was clear that there was a good agreement between the experimental points and predicted normalized concentration. The Thomas model is suitable for adsorption processes, where the external and internal diffusions are not the limited steps [29].

4.5.4. Yoon–Nelson model

A simple theoretical model developed by Yoon–Nelson was applied to investigate the breakthrough behavior of DO30 on the BMAC. So, the values of k_{YN} (a rate constant) and τ (the time required for 50% DO30 breakthrough) could be obtained using linear regressive analysis from Eq. (6). The values of K_{YN} and τ along with R^2 are listed in Table 3. The values of K_{YN} were found to decrease with an increase in both flow rate and bed height, whereas, the corresponding values of τ increased. With an increase in initial DO30 concentration, the K_{YN} values increased, whereas the τ values showed a reverse trend. From the experimental results and data regression, the model proposed by the Yoon–Nelson model provided a good correlation on the effects of influent DO30 concentration, flow rate, and bed depth.

Table 3
Kinetics model parameters obtained at different flow rates, inlet concentration and bed heights ($T = 26 \pm 2^{o}C$, pH = 6.3 ± 0.2)

Boharat–Adams model	$k_{AB,}$ L/mg min	$N_o \times 10^{-3}$ mg/L	R^2
Flow rate (mL/min)			
10	0.00026	44.613	0.54
20	0.000132	32.464	0.51
30	0.000103	17.981	0.54
Concentration (mg/L)			
50	0.0058	36.848	0.56
100	0.000212	15.674	0.62
200	8.15E-05	11.941	0.61
Bed height (mm)			
40	0.00012	27.983	0.75
60	0.000212	19.475	0.62
80	0.000237	15.796	0.64
BDST model	K, L/mg min	$N_o \times 10^{-3}$ mg/L	R^2
Flow rate (mL/min)			
10	1.111	34.431	0.92
20	1.253	21.845	0.97
30	0.909	17.186	0.98
Concentration (mg/L)			
50	0.585	24.513	0.89
100	0.558	17.225	0.94
200	0.501	12.115	0.97
Bed height (mm)			
40	1.012	8.852	0.96
60	1.111	17.301	0.94
80	1.42	15.536	0.91
Thomas model	k_{Th}, mL/min mg	q_o mg/g	R^2
Flow rate (mL/min)			
10	0.000827	46.01	0.96
20	0.000867	39.66	0.98
30	0.001133	29.72	0.98
Concentration (mg/L)			
50	0.000164	37.89	0.95
100	0.000491	25.96	0.96
200	0.000868	23.11	0.99
Bed height (mm)			
40	0.000864	39.47	0.98
60	0.000861	41.65	0.97
80	0.000749	91.97	0.98

(*Continued*)

Table 3 (*Continued*)

Yoon–Nelson model	k_{YN} L/min	τmin	R^2
Flow rate (mL/min)			
10	0.086	11.89	0.94
20	0.082	61.34	0.98
30	0.011	79.32	0.97
Concentration (mg/L)			
50	0.008	16.43	0.92
100	0.086	11.84	0.94
200	0.099	6.93	0.97
Bed height (mm)			
40	0.086	11.84	0.93
60	0.008	16.66	0.95
80	0.007	18.39	0.96

By comparing the values of R^2 listed in Table 3, for the whole breakthrough curves, the Yoon–Nelson model is a good fit to the relative concentration while the Thomas mode is the best fitted to the experimental data at various conditions up to 0.5 (C_t/C_o). Inspection of the regressed lines indicated that the model gave a good fit to the experimental data at all bed heights, flow rates, and influent DO30 concentrations and coefficient of determination, R^2 in the range of 0.95–0.99 (Table 3) and also good predictors for the breakthrough curve.

5. Conclusion

BMAC was found as an effective adsorbent for the efficient removal of DO30 from aqueous solutions in a fixed-bed column. The maximum removal of DO30 in a fixed-bed adsorption column was found as 39.97 mg/g at inlet concentration 100 mg/L, flow rate of 10 mL/min, and bed height 80 mm. The fixed-bed adsorption system was found to perform better with lower DO30 inlet concentration, lower feed flow rate, and higher activated carbon bed height. Predicted curves at various experimental conditions showed that the Thomas model was the most suitable for the tracing of a breakthrough curve at the experimental condition. The data were in good agreement with the Thomas model. The design of a continuous fixed-bed column treatment system for DO30 laden wastewater can be achieved by using the Thomas breakthrough models.

Acknowledgments

The authors acknowledge the research grant provided by University Science Malaysia under the RU Grant Scheme.

References

[1] U.G. Akpana, B.H. Hameed, Photocatalytic degradation of wastewater containing acid red 1 dye by titanium dioxide: Effect of calcination temperature, Desalin. Water Treat. 43 (2012) 84–90.
[2] A.A. Ahmad, B.H. Hameed, Effect of preparation conditions of activated carbon from bamboo waste for real textile wastewater, J. Hazard. Mater. 173 (2010) 487–493.
[3] M. Rafatullah, O. Sulaiman, R. Hashim, A. Ahmad, Adsorption of methylene blue on low-cost adsorbents: A review, J. Hazard. Mater. 177 (2010) 70–80.
[4] A.A. Ahmada, A. Idrisa, B.H. Hameed, Organic dye adsorption on activated carbon derived from solid waste, Desalin. Water Treat. 51 (2013) 2554–2563.
[5] O. Tunay, I. Kabdasli, D. Ohron, G. Cansever, Use and minimalization of water in leather tanning processes, Water Sci. Technol. 40(1) (1999) 237–244.
[6] K. Ivanov, E. Gruber, W. Schempp, D. Kirov, Possibilities of using zeolite as filler and carrier for dyestuffs in paper, Das Papier. 50 (1996) 456–460.
[7] R.V. Bhat, P. Mathur, Changing scenario of food colours in India, Curr. Sci. 74 (1998) 198–202.
[8] S.M.F. Cook, D.R. Linden, Use of rhodamine WT to facilitate dilution and analysis of atrazine samples in short-term transport studies, J. Environ. Qual. 26 (1997) 1438–1441.
[9] R.W. Wagner, J.S. Lindsey, Boron-dipyrromethane dyes for incorporation in synthetic multi-pigment light-harvesting arrays, Pure. Appl. Chem. 68 (1996) 1373–1380.
[10] D. Wrobel, A. Boguta, R.M. Ion, Mixtures of synthetic organic dyes in a photoelectronic cell, J. Photochem. Photobiol. A Chem. 138 (2001) 7–22.
[11] C. Scarpi, F. Ninci, M. Centini, C. Anselmi, High-performance liquid chromatography determination of direct and temporary dyes in natural hair colourings, J. Chromatogr. A 796 (1998) 19–25.
[12] S.S. Sahin, C. Demir, S. Guc, Simultaneous UV–vis spectrophotometric determination of disperse dyes in textile wastewater by partial least squares and principal component regression, Dyes Pigm. 73 (2007) 368–376.
[13] V. Golob, A. Ojstrsek, Removal of vat and disperse dyes from residual pad liquors, Dyes Pigm. 64 (2005) 57–61.
[14] B.H. Hameed, A.A. Ahmad, N. Aziz, Isotherms, kinetics and thermodynamics of acid dye adsorption on activated palm ash, Chem. Eng. J. 133 (2007) 195–203.

[15] S.T. Akar, R. Uysal, Untreated clay with high adsorption capacity for effective removal of C.I. Acid Red 88 from aqueous solutions: Batch and dynamic flow mode studies, Chem. Eng. J. 162 (2010) 591–598.
[16] Hatem A. AL-Aoha, M. Jamil Maaha, A.A Ahmadb, M. Radzi Bin Abasa, Adsorption of 4-nitrophenol on palm oil fuel ash activated by amino silane coupling agent, Desalin. Water Treat. 40 (2012) 159–167.
[17] C.Y. Li, W.G. Li, L. Wei, Research on absorption of ammonia by Nitric acid-modified Bamboo Charcoal at low temperature, Desalin. Water Treat. 47 (2012) 3–10.
[18] M. Lezehari, M. Baudu, O. Bouras, J.P. Basly, Fixed-bed column studies of pentachlorophenol removal by use of alginate-encapsulated pillared clay microbeads, J. Colloid Interface Sci. 379 (2012) 101–106.
[19] A.A. Ahmada, A. Idrisa, B.H. Hameed, Color and COD reduction from cotton textile processing wastewater by activated carbon derived from solid waste in column mode, Desalin. Water Treat. 41 (2012) 224–231.
[20] W. Li, Q. Yue, P. Tu, Z. Ma, B. Gao, J. Li, X. Xu, Adsorption characteristics of dyes in columns of activated carbon prepared from paper mill sewage sludge, Chem. Eng. J. 178 (2011) 197–203.
[21] K.S. Rao, S. Anand, P. Venkateswarlu, Modeling the kinetics of Cd(II) adsorption on Syzygium cumini L leaf powder in a fixed bed mini column, J. Ind. Eng. Chem. 17 (2011) 174–181.
[22] A.A. Ahmad, B.H. Hameed, Reduction of COD and color of dyeing effluent from a cotton textile mill by adsorption onto bamboo-based activated carbon, J. Hazard. Mater. 172 (2009) 1538–1543.
[23] Z. Aksu, F. Gonen, Biosorption of phenol by immobilized activated sludge in a continuous packed bed: Prediction of breakthrough curves, Process Biochem. 39 (2004) 599–613.
[24] G.S. Bohart, E.Q. Adams, Behavior of charcoal towards chlorine, J. Chem. Soc. 42 (1920) 523–529.
[25] R.A. Hutchins, New simplified design of activated carbon system, Am. J. Chem. Eng. 80 (1973) 133–138.
[26] V. Sarin, T.S. Singh, K.K. Pant, Thermodynamic and breakthrough column studies for the selective sorption of chromium from industrial effluent on activated eucalyptus bark, Bioresour. Technol. 97 (2006) 1986–1993.
[27] H.C. Thomas, Heterogeneous ion exchange in a flowing system, J. Am. Chem. Soc. 66 (1944) 1466–1664.
[28] Y.H. Yoon, J.H. Nelson, Application of gas adsorption kinetics. Part 1. A theoretical model for respirator cartridge service time, Am. Ind. Hyg. Assoc. J. 45 (1984) 509–516.
[29] R. Han, Y. Wang, Z. Xin, W. Yuanfeng, X. Fuling, C. Junmei, T. Mingsheng, Adsorption of methylene blue by phoenix tree leaf powder in a fixed-bed column: Experiments and prediction of breakthrough curves, Desalination 245 (2009) 284–297.
[30] Md.T. Uddin, Md. Rukanuzzaman, Md.M. Khan, Md. Akhtarul-Islam, Adsorption of methylene blue from aqueous solution by jackfruit (*Artocarpus heteropyllus*) leaf powder A fixed-bed column study, J. Environ. Manage. 90 (2009) 3443–3450.
[31] R. Han, D. Dandan, X. Yanfang, Z. Weihua, W. Yuanfeng, L. Yufei, Z. Lina, Use of rice husk for the adsorption of congo red from aqueous solution in column mode, Bioresour. Technol. 99 (2008) 2938–2946.
[32] W. Zhang, L. Dong, H. Yan, H. Li, Z. Jiang, X. Kan, H. Yang, A. Li, R. Cheng, Removal of methylene blue from aqueous solutions by straw based adsorbent in a fixed-bed column, Chem. Eng. J. 173 (2011) 429–436.
[33] A.A. Ahmad, B.H. Hameed, Fixed-bed adsorption of reactive azo dye onto granular activated carbon prepared from waste, J. Hazard. Mater. 175 (2010) 298–303.
[34] R. Han, L. Zou, X. Zhao, Y. Xu, F. Xu, Y. Li, Y. Wang, Characterization and properties of iron oxide-coated zeolite as adsorbent for removal of copper(II) from solution in fixed bed column, Chem. Eng. J. 149 (2009) 123–131.
[35] C.M. Futalana, C. Kanb, M.L. Dalidac, C. Pascuad, M.W. Wanb, Fixed-bed column studies on the removal of copper using chitosan immobilized on bentonite, Carbohydr. Polym. 83 (2011) 697–704.